

Parametric study and shrinkage modelling of natural rubber sheet drying using COMSOL multiphysics

C Ajani¹, A Kumar¹, S Curcio² and P Tekasakul¹

¹Energy Technology Research Center and Department of Mechanical, Engineering, Prince of Songkla University, Hat Yai, Songkhla 90112, Thailand

²Laboratory of Transport Phenomena and Biotechnology, Department of Computer Engineering, Modeling, Electronics and Systems, University of Calabria, 87036 Rende (CS), Italy

E-mail: clemajan@gmail.com

Abstract. Natural rubber is one of the major exporting cash crops in Thailand. Shrinkage in natural rubber sheet during drying creates uneven stresses in the rubber, hampers the quality and the water activity predisposes it to microbial activation. Hence, the effect of drying parameters on shrinkage has been considered in this work. The finite element concept coupled with the arbitrary Lagrangian-Eulerian (ALE) method was used to solve the two-dimensional coupled physics in the rubber sheet drying chamber and account for the shrinkage effect. The spatial domain (drying chamber), material domain (rubber sheet) was analysed. An isotropic linear elastic model was assumed for the rubber sheet for analysis. Three Case studies of different velocity, temperature, relative humidity and shrinkage coefficient were considered in the numerical study using COMSOL Multiphysics. It is concluded that increase in the operating parameters increases the shrinkage of the rubber. Therefore, rubber should dry at relatively lower operating parameters to improve its quality.

1. Introduction

Rubber sheets are important exporting product of Thailand. Thailand is the largest natural rubber (NR) producing and exporting country in the world at present. Total amount of NR products in year 2015, was around 4.5 million tons and the export was about 3.7 million tons, which accounted for 36% of global natural rubber production in same year. Commercially produced natural rubber is in the form of; ribbed smoked sheet (RSS), block rubber, rubber concentrated latex, and others [1]. Drying temperature, relative humidity, and air velocity, size of material, and initial moisture content are factors affect the quality of dried product, drying time and energy consumption. The optimization of rubber drying depends on four factors namely: drying temperature, relative humidity, and air velocity, and initial moisture content [2]. Optimization of the drying process and parameters is particularly required to enhance process efficiency in terms of energy usage and production time, without compromising the product quality (excessive shrinkage or Warping) [3]. Drying shrinkage can be defined as the volume reduction in porous materials such as rubber, concrete etc. suffers as a consequence of the moisture migration when exposed to a lower relative humidity environment than the initial one in its own pore system [4]. Simultaneous heat and moisture transfer accompanied by phase change, shrinkage, and/or absorption heat in some porous and composite materials (Rubber, concretes, wood) is a process, which occurs frequently in various engineering applications. Hassini et



al. reported that shrinkage effect cannot be neglected when moisture diffusivity in highly shrinking materials like natural rubber [5]. However, most of research on rubber drying solely considers the drying models without consideration of the rubber shrinkage during the drying process [6, 7, 8]. Shrinkage strongly depends on matrix mobility. It is proved that shrinkage is more significant during the constant and the falling rate periods, i.e. when matrix mobility is higher [9]. Katekawa and Silva, observed that shrinking in material volume actually corresponded to the volumetric amount of liquid water removed from the sample [10]. FEM is a versatile program applied in variety of engineering and science applications. Initially used in structural analysis, later gain relevance in multiphysics problems such as fluid structure interactions and other fluid flow problems such as complex industrial, mechanical, biomedical, aerospace applications etc. [11, 12, 13]. Perspective of the present work is to carry out a numerical study on the effect of operating parameters on the flow field and shrinkage of natural rubber sheet using COMSOL multiphysics.

2. Material and Method

2.1. Model Assumption

The basic assumptions in model formulation are: (a) The cubical symmetry, which restrict the analysis to a 2D geometry, (b) The natural rubber sheet sample is considered as a fictitious non-porous though it is a hygroscopic porous medium, (c) Transport in the sample is only a function of the water concentration, (d) Operating conditions in the chamber are assumed uniform, (e) Shrinkage characteristics are dependent on natural rubber moisture content.

2.2. Geometry and Material

A half 2D CAD geometry of the side view of the actual rubber drying chamber was designed in COMSOL Multiphysics v5.2 (Comsol AB, Stockholm, Sweden) as shown in figure 1. The same geometry is used for the simulation of the three sets of operating conditions. The side view as shown in figure 2 is considered for the shrinkage modelling. The labels 1, 2, 3 are the symmetry, 4 is the inlet, 5 is the outlet, 6 is the wall while 7, 8, 9 are the fluid structure boundary. The summary of the initial, boundary conditions and parameters used for the case studies are given in table 1, 2 and 3 respectively.

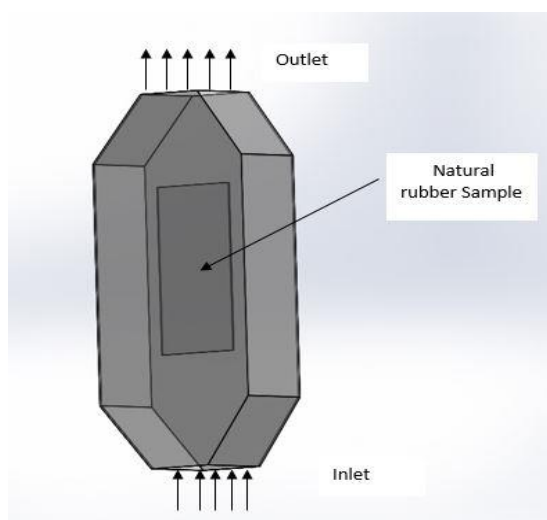


Figure 1. Schematic representation of the drying cell

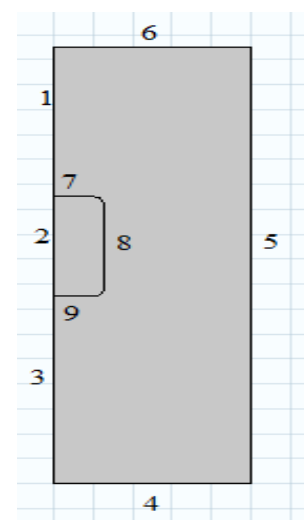


Figure 2. 2D geometry of drying cell

Table 1. Initial conditions used for the simulation

Medium	Variable	Value
Rubber	Moisture content on a dry basis (X_{b0})	4.06
Drying air	Temperature (T_0)	298 K
	Relative humidity (U_{x0})	50%
	Velocity in x and y directions (u_{x0}, u_{y0})	0 m/s
	Pressure in the drying chamber (P_0)	101, 325 Pa

Table 2. Boundary condition

Position	Transport	Expression
1, 2, 3	Symmetry	
4	Momentum	$u_x = 0, u_y = v_0$
	Heat	$T_2 = T_{air}$
	Mass	$C_2 = C_{air}$
5	Momentum	$\underline{u} / u_\tau = 1 / k \ln(\delta_w / l^*) + C^+$
	Heat	$T_2 = T_{air}$
	Mass	$C_2 = C_{air}$
6	Momentum	$p = p_{atm}$
	Heat	$\underline{n} \cdot (-k_a \underline{\nabla} T_2) = 0$
	Mass	$\underline{n} \cdot (-D_a \underline{\nabla} C_2) = 0$
7, 8, 9	Momentum	$\underline{u} / u_\tau = 1 / k \ln(\delta_w / l^*) + C^+$
	Heat	$T = T_{air}$
		$T = T_{air}$
	Mass	$C_2 = C_w$

Table 3. Operating parameters exploited for the simulation

Variable	Case A	Case B	Case C
Inlet Velocity (m/s)	0.5	1.0	1.5
Inlet Temperature (°C)	45	50	55
Inlet Relative humidity (%)	40	50	60

2.3. Governing Equations

The analysis is limited to a 2D due to complexity of the governing equation. The drying air/fluid model solved numerically incompressible Navier-Stokes equations along with the equations of momentum conservation, mass conservation, Energy balance, Mass balance as in equations (1), (2), (3) and (4) respectively [6, 7, 14].

$$\rho_a \frac{\partial \underline{\mathbf{u}}}{\partial t} + \rho_a (\underline{\mathbf{u}} \cdot \nabla) \underline{\mathbf{u}} = \nabla \left[-p \underline{\mathbf{I}} + \eta_a (\nabla \underline{\mathbf{u}} + (\nabla \underline{\mathbf{u}})^T) - 2/3 \eta_a (\nabla \cdot \underline{\mathbf{u}}) \underline{\mathbf{I}} \right] \quad (1)$$

$$\frac{\partial \rho_a}{\partial t} + \nabla \cdot (\rho_a \underline{\mathbf{u}}) = 0 \quad (2)$$

$$\rho_a C_{pa} \frac{\partial T_2}{\partial t} - \nabla \cdot (k_a \nabla T_2) + (\rho_a C_{pa} \underline{\mathbf{u}} \cdot \nabla T_2) = 0 \quad (3)$$

$$\frac{\partial C_2}{\partial t} + \nabla \cdot (-D_a \nabla C_2) + \underline{\mathbf{u}} \cdot \nabla C_2 = 0 \quad (4)$$

The transport in the rubber sheet is given by the mass balance equations in the rubber sample is as represented in equation (5) [13].

$$\frac{\partial C_w}{\partial t} + \nabla \cdot (-D_w \nabla C_w) + I = 0 \quad (5)$$

where, p is the pressure within the drying chamber (Pa), $\underline{\mathbf{u}}$ is the averaged velocity field (m/s), C_2 is water concentration in air (mol/m³), C_w is the water concentration in rubber (mol/m³), D_w is capillary diffusion coefficient of water in rubber (m²/s), I is volumetric rate of evaporation (mol/(m³ s)), T is air temperature (K), C_{pa} is the air specific heat (J/(kg K)), k_a is the air thermal conductivity (W/(m K)), ρ_a is air density (kg/m³), η_a is the air viscosity (Pa s), t is time (s), D_a is the diffusion coefficient of water in air (m²/s), and $\underline{\mathbf{I}}$ is the fluctuating part of velocity field (m/s).

The rubber is assumed to be undergoing an isotropic shrinkage. Local total strain $\{d\varepsilon\}$ is a function of the mechanical strain $\{d\varepsilon_s\}$ the shrinkage strain $\{d\varepsilon_0\}$ due to the moisture content.

$$\{d\varepsilon\} = \{d\varepsilon_s\} + \{d\varepsilon_0\} \quad (6)$$

Total strains $\{d\varepsilon\}$ is actually a function of the total displacement $\{dU\}$

$$\{d\varepsilon\} = [A]\{dU\}$$

$$\{d\varepsilon_0\} = K_{ds} \cdot dC_w$$

dC_w is the variation in the moisture content and the hydrous compressibility factor is K_{ds} which is estimated from the previous work [14]. The values of 6.01×10^{-6} , 7.01×10^{-6} , 8.01×10^{-6} was exploited for the three cases.

2.4. Physics and Mesh

The temperature and concentration are coupled to the laminar flow for the spatial domain. Solid mechanics is used for the material domain while ALE method is used to account shrinkage. Laplace smoothing, boundary and initial condition are applied. The solid and fluid domains are computationally meshed using COMSOL Multiphysics v5.2 (Comsol AB, Stockholm, Sweden). The

material and spatial domains are meshed using an extremely fine boundary layer mesh based on the COMSOL physics controlled mesh of minimum quality of 0.08.

2.5. Simulation Setup

The CFD simulations are solved by using commercial finite element solver, COMSOL Multiphysics 5.2 on a i5 dual-core computer. The solid mechanics and transport of diluted species module is used to solve the transport phenomena occurring in the rubber sheets to account shrinkage. Laminar flow module is exploited for solving the laminar flow as shown in equations (1) and (2). Equations (3) and (4) referred to the convection and conduction drying air was solved using heat transfer in fluids whereas the transport of diluted species module is used to solve equation (5). These equations are discretized using the second order for both the material and spatial frames. The relative and absolute tolerance are 0.01 and 0.001 respectively. Implicit time stepping scheme is used in the solution of the PDEs systems [14]. A combination of fully coupled and segregated solvers are applied in solving the time dependent study.

3. Result and Discussion

3.1. Flow behaviors at different operating parameters

The variation in the velocity flow patterns in the chamber for the three Cases are shown in figure 3(a), (b) and (c). Figure 3(c) shows the highest flow field and has more loading on the material domain. This is validated from previous research [14]. The coupled temperature and concentration in the drying chamber and the moisture content variation in the material domain for Case C are shown in figure 4(a), (b) and (c) respectively. Case C has the highest velocity, temperature and concentration variation in the drying chamber and thus could engender a faster evolution of moisture in the material domain of the three Case studies.

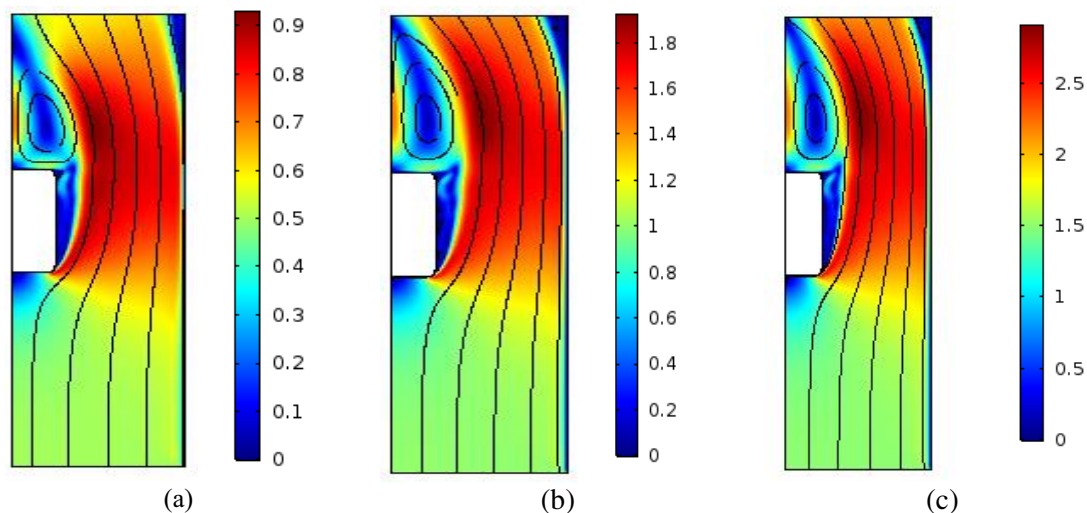


Figure 3. (a) Flow field for Case A, (b) Flow field for Case B (c) Flow field for Case C

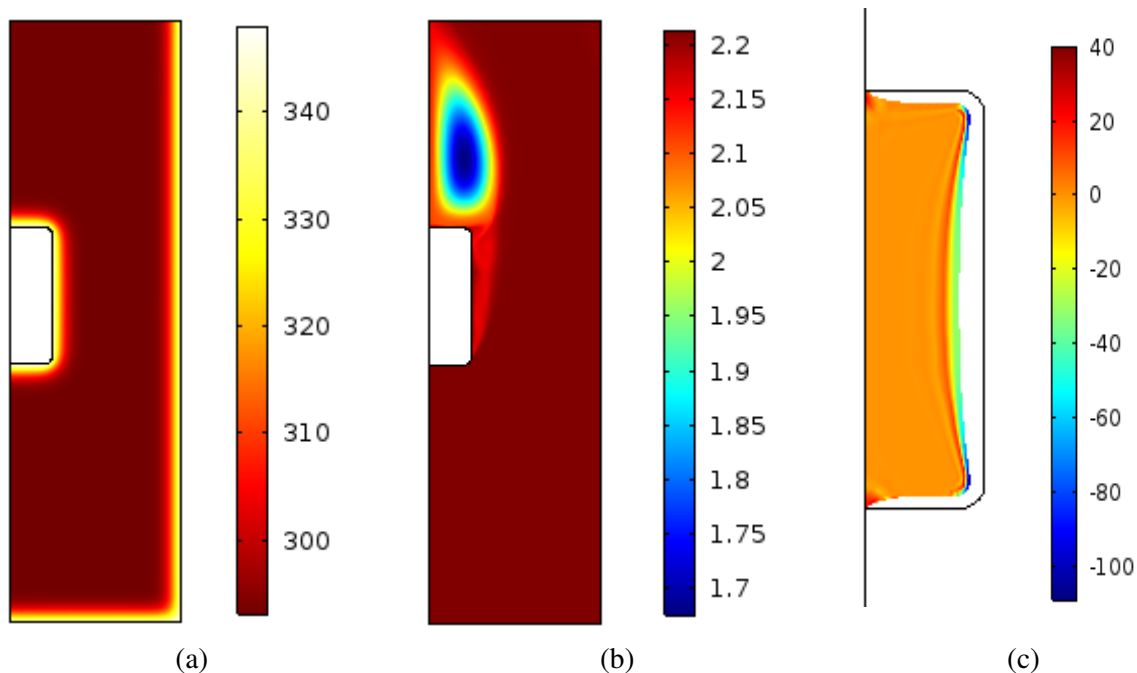


Figure 4. (a) Coupled temperature profile for Case C in the spatial domain (b) Coupled concentration profile for Case C in the spatial domain (c) Concentration profile for Case C in material domain

3.2. Shrinkage Behaviour

The von mises stress responsible for the shrinkage as shown in figure 5 (a), (b) and (c). Shrinkage followed a similar trend in all the Cases is also observed in same figure. This is due to an isotropic shrinkage model consideration. Figure 5 (c) has the highest shrinkage stress this mean, more strain on it. The horizontal shrinkage stress distributions from a 2D line plot at the height of 0.18m are shown in figure 6. The highest stresses are $1.96\text{e}8 \text{ N/m}^2$, $2.28\text{e}8 \text{ N/m}^2$ and $2.61\text{e}8 \text{ N/m}^2$ for all Cases A, B and C respectively. This implies that operating at higher operating parameter could engender higher shrinkage stress, thereby making the shrinkage more drastic and reducing the quality of the rubber. Although the rapid removal of the moisture content (at high operating condition) will reduce the predisposition of the rubber to microbial spoilage because of reduced water activity. This is similar with previous research on convective drying of porous agricultural products with shrinkage effect [14, 15], therefore model is validated.

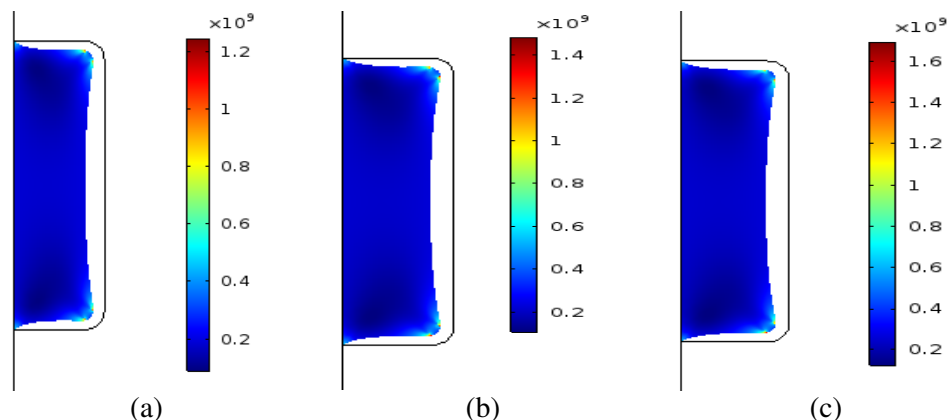


Figure 5. (a) Von mises shrinkage stress for Case A (b) Von mises shrinkage stress for Case B (c) Von mises shrinkage stress for Case C.

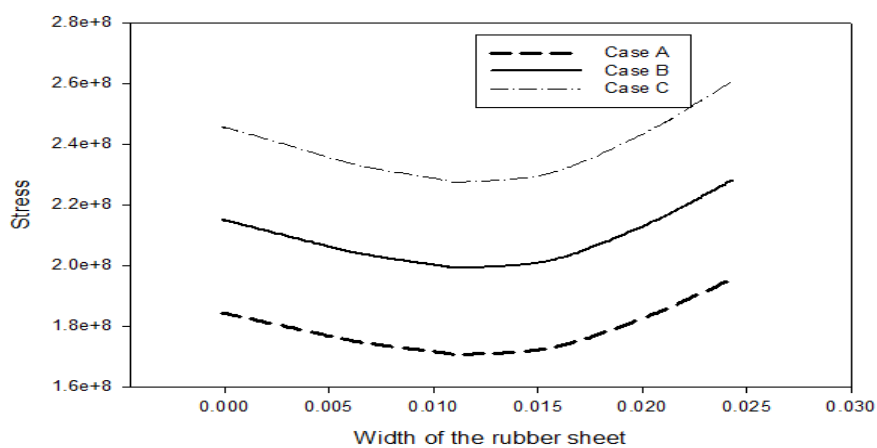


Figure 6. Shrinkage stress distribution on width of material at 0.18m height

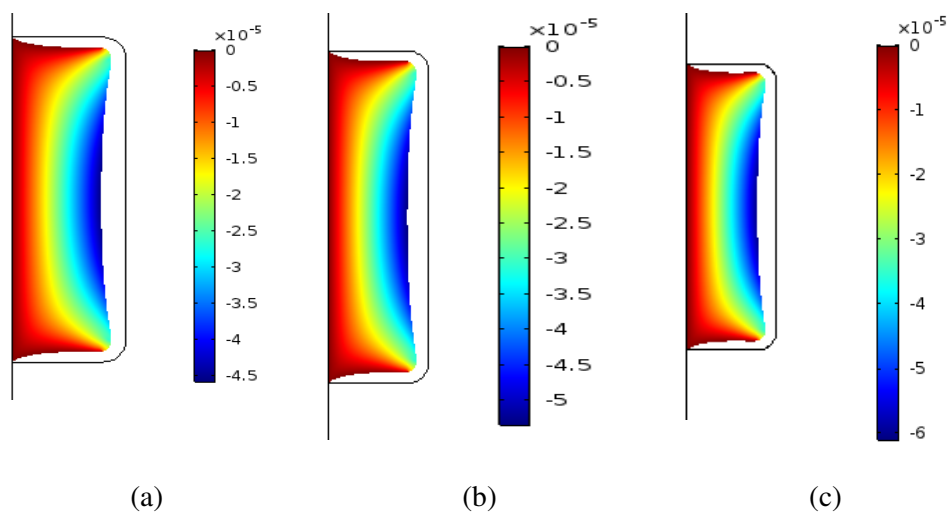


Figure 7. Shrinkage strain / displacement

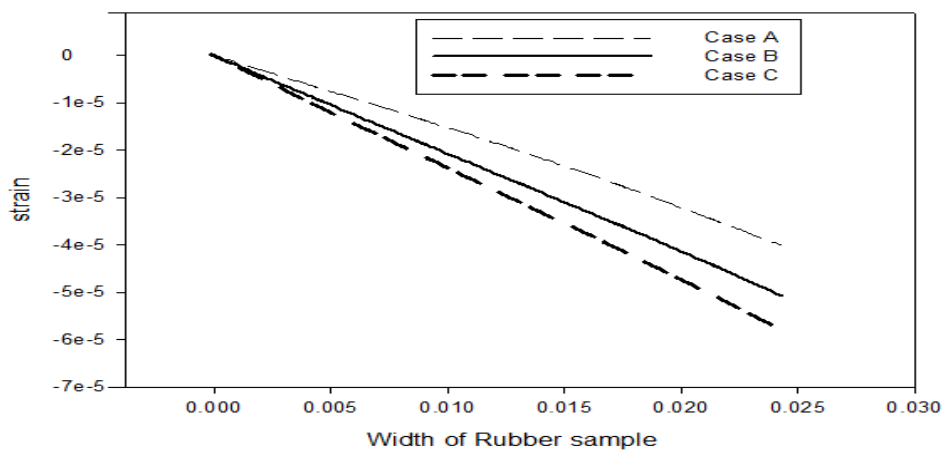


Figure 8. Shrinkage strain distribution on width of material at 0.18m height

Figure 7 (a), (b) and (c) show the resulting shrinkage strains /displacements due to the applied stresses in all Cases. It is observed that Case A has the least shrinkage while Case C has the highest shrinkage. A 2D line plot of the displacements /shrinkages of the rubber from their initial width at height 0.18m are shown in figure 8. The nature of the graphs for the three case studies further explains the shrinkage behaviours. The highest displacement/ shrinkage from the initial width at height 0.18m are $-4.0264\text{e-}5\text{m}$, $-5.0702\text{e-}5\text{m}$ and $-5.7943\text{e-}5\text{m}$ for Cases A, B and C respectively. The stresses developed in C is the highest as shown in figure 6, hence, the highest shrinkage/ displacement of $-5.7943\text{e-}5\text{m}$ as shown in figure 8. The shrinkage in A is the milder compared to the others because of it reduced operating conditions.

4. Conclusion

A predictive model to study the effects of operating conditions and rubber mechanical properties on rubber shrinkage drying using COMSOL Multiphysics was formulated. The ALE method with the relevant domain integration was used to solve the equations. The obtained results confirmed that it is crucial to develop a model capable of predicting the actual variation of natural rubber shape and dimensions. This shows that deformation strongly influenced the transport phenomena and hence, cannot be neglected. The proposed approach is capable to calculate the effect of different variables, which could be used to ascertain either the natural rubber safety in terms of the microbial inactivation kinetics based on the water activity or the quality index based on the shrinkage stress distribution.

Acknowledgement

This research was supported by Higher Education Research Promotion and the Thailand's Education Hub for Southern Region of ASEAN Countries Project Office of Higher Education Commission. This research was also supported by Natural Rubber Innovation Research Institute, Prince of Songkla University (Grant No. ENG590305S).

References

- [1] Agricultural Statistics of Thailand 2016 *Ministry of Agriculture & Co-Operatives, Bangkok, Thailand*
- [2] Theppaya T and Prasertsan S 2004 *Dry. Technol.* 22 1637–60
- [3] Kowalski S J and Pawlowski A 2011 *Chem. Eng. Sci.* 66 1893–905
- [4] P. Mehta P M 2005 *Concrete: Microstructure, Properties, and Materials* 684
- [5] Hassini L, Azzouz S, Peczkalski R and Belghith A 2007 *J. Food Eng.* 79 47–56
- [6] Promtong M and Tekasakul P 2007 *Appl. Therm. Eng.* 27 2113–21
- [7] Tekasakul P, Dejchanchaiwong R, Tirawanichakul Y and Tirawanichakul S 2015 *Dry. Technol.* 33 1124–37
- [8] Dejchanchaiwong R, Tirawanichakul Y, Tirawanichakul S, Kumar A and Tekasakul P 2017 *Appl. Therm. Eng.* 112 761–70
- [9] Karathanos V T and Belessiotis V G 1996 *J. Food Eng.* 29 167–83
- [10] Katekawa M E and Silva M A 2007 *Dry. Technol.* 25 1659–66
- [11] Bathe K-J 2006 *Finite element procedures* (Watertown, MA)
- [12] Zienkiewicz O C and Taylor R L 2000 *The Finite Element Method Volume 1: The Basis Methods* (Butter Heinemann) p708
- [13] Bathe K J and Saunders H 1984 *J. Press. Vessel Technol.* 106 421
- [14] Curcio S and Aversa M 2014 *J. Food Eng.* 123 36–49
- [15] Curcio S and Aversa M 2009 *COMSOL Conf.* (Milán)